

Accepted Manuscript

Experimental investigation of the phase equilibria of the Al-Ca-Zn system at 623 K

D. Kevorkov, Y.N. Zhang, K. Shabnam, P. Chartrand, M. Medraj

PII: S0925-8388(12)00998-X

DOI: <http://dx.doi.org/10.1016/j.jallcom.2012.06.029>

Reference: JALCOM 26477

To appear in:

Received Date: 20 February 2012

Revised Date: 1 June 2012

Accepted Date: 6 June 2012

Please cite this article as: D. Kevorkov, Y.N. Zhang, K. Shabnam, P. Chartrand, M. Medraj, Experimental investigation of the phase equilibria of the Al-Ca-Zn system at 623 K, (2012), doi: <http://dx.doi.org/10.1016/j.jallcom.2012.06.029>

This is a PDF file of an unedited manuscript that has been accepted for publication. As a service to our customers we are providing this early version of the manuscript. The manuscript will undergo copyediting, typesetting, and review of the resulting proof before it is published in its final form. Please note that during the production process errors may be discovered which could affect the content, and all legal disclaimers that apply to the journal pertain.



Experimental investigation of the phase equilibria of the Al-Ca-Zn system at 623 K

D. Kevorkov¹, Y.N. Zhang¹, K. Shabnam¹, P. Chartrand², M. Medraj^{1*}

¹Department of Mechanical Engineering, Concordia University,
1455 de Maisonneuve Blvd. W., Montreal, Quebec, CANADA, H3G 1M8

²Centre for Research in Computational Thermochemistry, Department of Chemical Engineering,
Ecole Polytechnique, Montreal, Quebec, CANADA, H3C 3A7

Abstract

The Al-Ca-Zn phase diagram at 623 K was experimentally studied using diffusion couples and selected key alloys. Three new ternary compounds IM1 (with the composition range of $\text{Al}_{30}\text{Ca}_8\text{Zn}_{62}$ to $\text{Al}_{27}\text{Ca}_8\text{Zn}_{65}$), IM2 (with the composition range of $\text{Al}_{25}\text{Ca}_{25}\text{Zn}_{50}$ to $\text{Al}_{20}\text{Ca}_{25}\text{Zn}_{55}$) and IM3 ($\text{Al}_{15}\text{Ca}_{63}\text{Zn}_{22}$) have been found in this system. In addition, the existence of two ternary compounds: C36 and Al_2CaZn_2 were confirmed. Their solubility at 623 K was found to be: C36 (from $\text{Al}_{58}\text{Ca}_{33}\text{Zn}_9$ to $\text{Al}_{43}\text{Ca}_{33}\text{Zn}_{24}$) and Al_2CaZn_2 (from $\text{Al}_{55}\text{Ca}_{20}\text{Zn}_{25}$ to $\text{Al}_{40}\text{Ca}_{20}\text{Zn}_{40}$). Ternary solubility of the binary compounds was determined. Based on the current results and experimental literature data, the isothermal section of the Al-Ca-Zn phase diagram at 623 K was constructed.

Keywords: Intermetallics; Phase diagrams; Microstructure; X-ray diffraction; Electron microscopy

1. Introduction

Aluminum and its alloys are the primary structural material used in aircraft industry. The combination of acceptable cost, good mechanical properties, low density, good creep resistance, structural integrity and ease of fabrication makes them attractive for various industrial applications. The intensive research is ongoing on the improvement of mechanical properties of aluminum alloys [1-4]. The Al-Ca-Zn alloys exhibit superplastic behavior [5-7] and, therefore, have attracted much attention in recent years. For instance, an Al alloy containing 5 wt.% Ca and 5 wt.% Zn shows superplastic forming behavior at room temperature [6]. Therefore, understanding the equilibrium phase relationships in the Al-Ca-Zn ternary system is essential for further development of these alloys. Another useful and important application of the Al alloys containing Ca and Zn is in corrosion protection [8]. These protectors were characterized by high current efficiency and long service life. Therefore, they have been used for the protection of underground and underwater pipelines, reservoirs, oil storages, drilling rigs, municipal communications and continental shelf structures [8].

2. Literature review

The Al-Ca-Zn system was experimentally investigated by several researchers [6, 9-15]. Despite of the extensive study, some of the results were contradictory. Moore and Morris [6] first investigated the Al-Ca-Zn system in the Al-rich corner and discovered a new ternary compound Al_3CaZn using metallography, differential thermal analysis, electron probe micro-analysis (EPMA), transmission electron microscopy (TEM) and x-ray diffraction (XRD) techniques. They [6] also reported this compound to be superplastic and have a body centered tetragonal structure. Later, Kono et al. [9] studied the Al-Ca-Zn system and confirmed formation of the Al_3CaZn ternary compound using micrography, inverse rate thermal analysis, x-ray diffraction and EPMA analysis. Also, Kono et al.

[9] reported that the Al_4Ca binary compound gradually changes into a ternary compound Al_3CaZn . Almost at the same time Cordier et al. [10] reported that the crystal structure of a new ternary compound Al_2CaZn_2 has an ordered ternary superstructure of Al_4Ba -type structure. Later, Ganiev et al. [11] determined the isothermal section of the Al-Ca-Zn system at 623 K using x-ray diffraction and metallographic examination. They also reported the congruent melting temperatures of the Al_2CaZn_2 ternary compound at 1113 K using differential thermal analysis (DTA). The presence of this compound was later confirmed by Gantsev et al. [12]. Recently, Pani et al. [13] reported a wide homogeneity range for Al_4Ca up to $\text{Al}_{1.88}\text{CaZn}_{2.12}$ at 823 K. The general formula for this compound was proposed as $\text{Ca}(\text{Zn}_{1-x}\text{Al}_x)_4$ ($x=0.47-1.00$ at 823 K) with an Al_4Ba structure type, which includes the ternary composition Al_2CaZn_2 . However, phase relations among Al_4Ca , Al_3CaZn and Al_2CaZn_2 phases were not clearly described in the literature [6, 9-13]. In addition, a number of researchers [9, 11, 12, 14, 15] reported AlCaZn ternary compound, but their results were contradictory. Kono et al. [9] reported that Al is substituted by Zn in the Al_2Ca binary compound until the ternary compound AlCaZn forms. Ganiev et al. [11] and Gantsev et al. [12] reported that AlCaZn phase melts congruently at 1263 K based on the differential thermal analysis data and metallography. Later Söderberg et al. [14] and Pani et al. [15] studied the Al_2Ca - CaZn_2 pseudobinary section, reporting that the Al_2Ca binary compound has a ternary solubility up to 6 at% Zn. Both Söderberg et al. [14, 16] and Pani et al. [15] reported a new ternary C36 Laves phase with a composition $\text{Al}_{2-x}\text{CaZn}_x$ ($0.28 \leq x \leq 0.68$) that forms peritectically at 1227 K. Pani et al. [15] used x-ray single crystal diffractometry to confirm the C36 structure (MgNi₂-type) for the $\text{Al}_{1.406}\text{CaZn}_{0.594}$ composition. According to the work of Söderberg et al. [14], the AlCaZn phase has the KHg_2 -structure and is a part of the CaZn_2 solid solution, which forms peritectically from the C36 phase at 1112 K. This result was also confirmed by Pani et al. [15] by EPMA and single crystal x-ray diffraction at 973 K. Later, Pani et al. [13] investigated the Al-Ca-Zn system from 8 to 33 at% Ca at 823 K by optical and

scanning electron microscopy (SEM), EPMA and XRD. They reported several binary phases with their homogeneity ranges and crystal structures: $\text{Ca}(\text{Zn}_{1-x}\text{Al}_x)_3$ ($x = 0 - 0.23$, CaZn_3 type), $\text{Ca}(\text{Zn}_{1-x}\text{Al}_x)_4$ ($x = 0.47 - 1.00$, BaAl_4 type), $\text{Ca}_{1-y}(\text{Zn}_{1-x}\text{Al}_x)_{5+2y}$ ($x = 0 - 0.12$ and $y = 0 - 0.12$, CaCu_5 -derived TbCu_7 type), $\text{Ca}(\text{Zn}_{1-x}\text{Al}_x)_{11}$ ($x = 0 - 0.018$, BaCd_{11} type). They also reported the $\text{Ca}_2(\text{Zn}_{1-x}\text{Al}_x)_{17}$ ($x = 0.05 - 0.17$, $\text{Th}_2\text{Zn}_{17}$ type) ternary phase.

Wendroff and Röhr [17] reported that the CaZn_5 binary compound has a solubility range 14.3-16.7 at.% Ca, corresponding to the change of the stoichiometry from 1:5 to 1:6 with a continuous structural change from CaCu_5 to TbCu_7 . This data agrees with the work of Pani et al. [13], who observed the same phenomenon in the ternary system, and reported CaZn_5 as a solid solution where Ca substitutes Zn/Al-Zn/Al pairs resulting in decrease in the lattice parameter, whereas the substitution of the Zn atom for Al generates an increase. They formulated this binary compound with ternary solubility as $\text{Ca}_{1-y}(\text{Zn}_{1-x}\text{Al}_x)_{5-2y}$ ($x = 0-0.12$ and $y = 0-0.12$, CaCu_5 - derived TbCu_7 type). The Al-Ca-Zn ternary system was thermodynamically modeled by Wasiur-Rahman [18, 19] using the modified quasicheical model. The authors considered the presence of only two ternary compounds, AlCaZn and Al_2CaZn_2 . Unfortunately, the ternary solubility of binary compounds was not modeled and other experimental data on this system appeared after their work was published. Therefore, this system has to be remodeled taking into consideration the new experimental findings. Despite of the large amount of experimental data, no systematic experimental study of the Al-Ca-Zn system could be found in the literature. Many phase relations were unclear and the information on the phase compositions was contradictory as illustrated in Fig. 1. Experimental results of the Al-Zn rich side of the Al-Ca-Zn isothermal section at 623 K were presented in this work.

Fig. 1. Graphical summary of the literature data.

3. Experimental

The isothermal section of the Al-Ca-Zn system at 623 K was studied experimentally using 5 diffusion couples and 26 key alloys. The assessment of the literature data was taken as a basis for the experimental study. The starting materials were 99.999% pure Al, 99.99% pure Zn and 99% pure Ca supplied by Alfa-Aesar. The alloys were prepared in an arc-melting furnace with water-cooled copper crucible in an argon atmosphere using a non-consumable tungsten electrode. All the samples were re-melted 5 times in the arc-melting furnace to ensure homogeneity. To compensate for the mass loss of Ca and Zn due to their high vapor pressure, extra 5 and 8 weight percentages of Ca and Zn, respectively, were added to the compositions before melting. The global actual compositions of the prepared samples were then determined by inductively coupled plasma (ICP) after melting. The actual composition was used for the analysis. The samples were sealed in quartz tubes under Ar atmosphere and annealed at 623 K.

Four solid-state diffusion couples (SSDC) and one solid-liquid diffusion couple (SLDC) were prepared in this work. The faces of the end members of the solid-solid diffusion couples were pre-grounded up to 1200 grit using SiC paper and polished up to 1 μ m using diamond suspension and 99% ethanol as lubricant. The pieces were then pressed together using clamping rings, wrapped in a tantalum foil, sealed in a quartz tube under protective argon atmosphere. Finally the diffusion couples were annealed at 623 K for 5 weeks and quenched in cold water. The compositions of the solid-solid diffusion couples were: SSDC-1: Al₆₆Ca₂₇Zn₇-Zn; SSDC-2: Al₇₀Ca₁₂Zn₁₈-Zn; SSDC-3: Al₄₀Ca₄₀Zn₂₀-Zn; SSDC-4: Al₃₀Ca₃₇Zn₃₃-Zn. The composition of the solid-liquid diffusion couple was Al₂Ca-Zn.

To prepare the Al₂Ca-Zn solid-liquid diffusion couple, a piece of Zn was melted on top of the higher melting temperature Al₂Ca part in the arc-melting furnace under protective argon atmosphere. The sample was then sealed in a quartz tube and annealed for one week at 623 K followed by quenching in water.

Diffusion couples and key alloys were analyzed by EPMA and XRD. The microstructure, compositions, layer thickness (in case of the diffusion couples) and homogeneity ranges of the phases were determined by quantitative EPMA analysis. For this purpose, EPMA (JEOL-JXA-8900) with a 2 μ m probe diameter, 15kV accelerating voltage, 20nA probe current has been used. The error of the EPMA measurements was estimated to be about ± 2 at.%. This value was obtained from the comparison and statistical analysis of the compositions of selected phases from several samples. The phases and their compositions were identified using EPMA with point and line scans.

The XRD patterns were obtained using PANalytical X'pert Pro powder x-ray diffractometer with a CuK α radiation. The XRD spectrum was acquired from 20 $^\circ$ to 120 $^\circ$ with a step size 0.02 $^\circ$ and a scanning time 14s/step. X-ray diffraction study of the samples was done using X'Pert High Score Plus Rietveld analysis software in combination with Pearson's crystal database [20].

4. Results and discussion

The Al-Ca-Zn system at 623 K was studied in this work. The analysis of the diffusion couples was used to determine the main phase relations in this system. The unclear or missing tie-lines were verified by the key-alloys.

The microstructure of the solid-solid diffusion couple SSDC-1 with increased magnification of the area of interest is illustrated in Fig. 2. As shown in Fig. 2(a), several multiphase diffusion layers were formed in this diffusion couple. The compositions of the formed phases were detected by the EPMA point analysis. The EPMA line scans were used to determine the solubility ranges and phase equilibria among intermetallics. The same approach was used to study other diffusion couples.

A new ternary compound was detected in this diffusion couple. It is denoted as IM1 in this work. The composition inferred from the EPMA results is $Al_xCa_8Zn_y$ ($28 \leq x \leq 29$, $62 \leq y \leq 65$). As shown in Fig. 2(b), the IM1 phase is in equilibrium with Al_2CaZn_2 and $CaZn_{13}$ compounds. The binary compound $CaZn_{13}$ has a maximum solubility of 9.1 at.% Al. The Al-fcc miscibility gap was detected in this diffusion couple and illustrated in Fig. 2(c). The phase equilibrium between Al_4Ca and Al_2CaZn_2 compounds is shown in Fig. 2(d).

Fig. 2. Back-scattered electron image of SSDC-1 annealed at 623 K for 5 weeks.

Part of the solid-state diffusion couple SSDC-2 that illustrates formation of the diffusion layers is presented in Fig. 3. The presence of the IM1 compound was confirmed in this diffusion couple. The following phase equilibria were detected in this diffusion couple: $(Al_2Ca)-(Al_4Ca)$, $(Al_4Ca)-(Al_2CaZn_2)$, $(Al_2CaZn_2)-(IM1)$, $(IM1)-fcc\ Al\ (Al\text{-rich})$, $(IM1)-(CaZn_{13})$, $fcc\ Al\ (Al\text{-rich})-(CaZn_{13})$, $fcc\ Al\ (Al\text{-rich})-fcc\ Al\ (Zn\text{-rich})$, $fcc\ Al\ (Zn\text{-rich})-(CaZn_{13})$, $(CaZn_{13})-Zn$.

Fig. 3. Back-scattered electron image of SSDC-2 at 623 K annealed for 5 weeks.

A 45 μ m EPMA line scan was carried out to find the homogeneity ranges of Al₄Ca, Al₂CaZn₂, IM1 and CaZn₁₃ phases and phase equilibria among them. The two phase region between Al₄Ca and Al₂CaZn₂ was clearly established as shown in Fig. 3. This finding proves that Al₄Ca and Al₂CaZn₂ are two separate phases at 623 K and contradicts the data of Pani et al. [13] who reported a continuous solid solution Ca(Zn_{1-x}Al_x)₄ (x=0.47-1.00) at 823 K. However, it is possible that the continuous solid solution at 823 K decomposes before reaching 623 K to Al₄Ca and Al₂CaZn₂ phases, suggesting the presence of solid state immiscibility gap. This assumption is supported by two facts: (i) Al-Zn system demonstrates similar tendency for the Al-fcc phase and (ii) Al₄Ca and Al₂CaZn₂ phases have related crystal structures that can form continuous solid solubility. Additional experimental study is needed to verify this assumption. The Al₄Ca solid solution has the maximum solubility of 15 at% Zn at 623 K. The solid solubility limit of Al₂CaZn₂ phase in equilibrium with Al₄Ca (shown in Fig. 3(b)) was found to be Al₅₅Ca₂₁Zn₂₄ at 623 K.

The composition of the IM1 compound was determined to be Al₃₁Ca₈Zn₆₁ at the boundary with Al₂CaZn₂. Based on the two phase equilibrium between IM1 and CaZn₁₃, the Zn-rich boundary of the IM1 was determined to be Al₂₄Ca₈Zn₆₈ and the maximum ternary solubility of the CaZn₁₃ compound was found to be 8.3 at.% Al. Taking into account that the maximum solubility of the CaZn₁₃ phase in SSDC-1 was 9.1 at.% Al and the estimated error of measurement of EPMA ± 2 at.%Al, we can state that a good agreement between these data (difference below 1 at.%Al) is obtained.

The microstructure showing part of SSDC-3 is illustrated in Fig. 4. Four ternary compounds were found in this diffusion couple: IM2, IM3, Al₂CaZn₂ and C36. The binary compounds: CaZn₂, CaZn₅, CaZn₁₁ and CaZn₁₃ have extended solid solubility in the ternary system. The following three phase

triangulations were identified from SSDC-3 shown in Fig. 4: IM2, C36 and Al_2CaZn_2 ; IM2, C36 and (CaZn_2) ; IM2, Al_2CaZn_2 and (CaZn_5) ; Al_2CaZn_2 , (CaZn_5) and (CaZn_{11}) . The homogeneity ranges of C36 and (CaZn_2) were studied using EPMA point analysis at the two phase boundary. The maximum solubility of C36 in the Zn-rich side and (CaZn_2) in the Al-rich side was determined to be $\text{Al}_{43}\text{Ca}_{33}\text{Zn}_{24}$ and $\text{Al}_{35}\text{Ca}_{33}\text{Zn}_{32}$ respectively. These results are in good agreement with the values reported by [14, 15]: C36 ($\text{Al}_{44}\text{Ca}_{33}\text{Zn}_{23}$) and CaZn_2 ($\text{Al}_{34}\text{Ca}_{33}\text{Zn}_{33}$). The limit of Al_2CaZn_2 solid solution was found from $\{\text{Al}_2\text{CaZn}_2, (\text{CaZn}_5) \text{ and } (\text{CaZn}_{11})\}$ triangulation. It has an $\text{Al}_{40}\text{Ca}_{20}\text{Zn}_{40}$ composition in the Zn-rich side. Two new ternary compounds were found from this diffusion couple by EPMA point analysis: $\text{Al}_{20}\text{Ca}_{25}\text{Zn}_{55}$ (IM2) and $\text{Al}_{14}\text{Ca}_{63}\text{Zn}_{23}$ (IM3). To determine the homogeneity range of IM2, several key alloys were analyzed and will be discussed below. The CaZn_5 compound has a ternary extension of the solid solubility up to 11.3 at% Al. The ternary solubility of the CaZn_{11} compound was found to be 1.7 at% Al. The composition of the eutectic region in the Zn-rich zone of the diffusion couple is $\text{Al}_{16}\text{Ca}_{13}\text{Zn}_{71}$.

Fig. 4. Back-scattered electron image of SSDC-3 at 623 K annealed for 5 weeks.

Nine different intermetallic compounds form in SSDC-4. A part of SSDC-4 is presented in Fig. 5. Four ternary compounds IM2, IM3, Al_2CaZn_2 , C36 and five binary compounds $\text{Al}_{14}\text{Ca}_{13}$, CaZn_2 , CaZn_5 , CaZn_{11} , and CaZn_{13} were found in this diffusion couple. All binary compounds have extended solid solubilities in the ternary. The following phase triangulations were identified in SSDC-4: IM3, $(\text{Al}_{14}\text{Ca}_{13})$, (CaZn_2) ; C36, $(\text{Al}_{14}\text{Ca}_{13})$, (CaZn_2) ; C36, (IM2), (CaZn_2) ; IM2, Al_2CaZn_2 , C36; IM2, Al_2CaZn_2 , (CaZn_5) ; Al_2CaZn_2 , (CaZn_{11}) , (CaZn_{13}) . The homogeneity ranges of different binary and ternary compounds were detected by EPMA spot and line scans. The solubility limit of the Al-rich side of the C36-phase was determined as $\text{Al}_{57}\text{Ca}_{33}\text{Zn}_{10}$, which is in a good agreement

with the values reported by [14, 15]: $\text{Al}_{58}\text{Ca}_{33}\text{Zn}_9$. The maximum solubility of Al_2CaZn_2 was found to be $\text{Al}_{40}\text{Ca}_{20}\text{Zn}_{40}$ in the Zn-rich side. The composition of IM2 was determined to be $\text{Al}_{20}\text{Ca}_{25}\text{Zn}_{55}$ by EPMA point analysis while the composition of IM3 was detected as $\text{Al}_{15}\text{Ca}_{63}\text{Zn}_{22}$. The $\text{Al}_{14}\text{Ca}_{13}$ compound has a ternary solubility limit up to 17 at% Zn. The ternary extension of the CaZn_2 solid solution was detected to be 31 at% Al, which is lower than what was observed in SSDC-3 (34 at% Al). The solid solutions of CaZn_5 and CaZn_{13} have maximum ternary solubilities of up to 9 at% Al.

Fig. 5. Back-scattered electron image of SSDC-4 at 623 K annealed for 5 weeks.

The production of some solid-solid diffusion couples was limited because of the brittleness of the end members. Therefore, solid-liquid diffusion couple with the end members Al_2Ca and Zn was prepared and annealed at 623 K for 1 week. Its microstructure is illustrated in Fig. 6. This Fig. 6 also presents the compositional profile of the line scan and its projection on the Gibbs triangle. The analysis of the diffusion couple has revealed several zones along the diffusion path: $\text{Al}_2\text{Ca} \rightarrow \text{Al}_4\text{Ca} \rightarrow \text{Al}_2\text{CaZn}_2 \rightarrow (\text{IM1} + \text{fcc Al-1}) \rightarrow (\text{fcc Al-1} + \text{fcc Al-2} + \text{CaZn}_{13}) \rightarrow \text{Zn}$. Two ternary intermetallic compounds were found in this diffusion couple: Al_2CaZn_2 and IM1. The solid solubility of the IM1 phase was found to be between 27 and 29 at% Al at constant Ca content 9 at% Ca. The analysis of the Al_4Ca - Al_2CaZn_2 two phase equilibrium determined the solubility limit of the Al_4Ca (16 at% Zn) and the Al-rich boundary of the Al_2CaZn_2 phase (56 at% Al). The obtained values are in good agreement with the SSDC-2. The ternary solubility of CaZn_{13} was found to be 9 at% Al confirming the results from SSDC-4.

Fig. 6. Backscattered electron image of solid-liquid diffusion couple Al_2Ca -Zn at 623 K annealed for 5 weeks. Points in brackets are offsets.

Combining the results obtained from four solid-solid diffusion couples and one solid-liquid diffusion couple, a partial isothermal section of the Al-Ca-Zn system at 623 K was constructed. Three new ternary phases IM1, IM2 and IM3 were found and two known phases C36 and Al_2CaZn_2 were confirmed. Also the ternary solubilities of binary compounds were detected. Unfortunately, just the major phase relations were determined using diffusion couples. In order to improve the understanding of the ternary phase diagram, 26 key alloys were prepared and studied. They were used to determine the solubility ranges of ternary and binary phases and for the determination of the missing phase relationships. All the samples were studied by EPMA and XRD to compare and cross-check the experimental results from different methods and to establish correct phase equilibria. An example of the phase analysis is given in Fig. 7.

Fig. 7. Phase analysis of $\text{Al}_{13}\text{Ca}_{17}\text{Zn}_{70}$ sample using EPMA and XRD results.

The phase analysis results of the key samples were projected on the solid solubilities detected using diffusion couples as presented in Fig. 8. Based on the phase analysis of the key alloys and diffusion couples, solubility limits of the binary and ternary phases were determined as well as the two- and three-phase regions. The solubility ranges of binary and ternary phases are given in Table 1.

Fig. 8. Phase analysis of key samples projected on the solid solubilities detected using diffusion couples.

Table 1. Experimental solid solubilities in the Al-Ca-Zn system at 623 K.

The detected solid solubilities have a good correlation with the published literature data. Since this study was carried out at lower temperature than reported in the literature, the direct comparison was not possible. Therefore, the pseudobinary $\text{Al}_2\text{Ca}-\text{CaZn}_2$ phase diagram was constructed using data of Söderberg et al. [14] and the current experimental data. As illustrated in Fig. 9, this work is in excellent agreement with the data of Söderberg et al. [14].

Fig. 9. The pseudobinary $\text{Al}_2\text{Ca}-\text{CaZn}_2$ phase diagram constructed using data of Söderberg et al. [14] and our experimental data.

Based on current findings, the isothermal section of the Al-Ca-Zn ternary system at 623 K was constructed below 50 at.% Ca. The Ca-rich part of the phase diagram was estimated based on the binary phase diagrams and limited ternary data. The resulted isothermal section is illustrated in Fig. 10.

Fig. 10. The isothermal section of the Al-Ca-Zn system at 623 K.

5. Conclusions

The isothermal section of the Al-Ca-Zn phase diagram at 623 K was constructed using diffusion couples and selected key alloys. The homogeneity ranges of ternary and binary compounds were determined and the phase relations among them were established using the EPMA and XRD studies.

Three new ternary compounds IM1 ($\text{Al}_{30}\text{Ca}_8\text{Zn}_{62}$ - $\text{Al}_{27}\text{Ca}_8\text{Zn}_{65}$), IM2 ($\text{Al}_{25}\text{Ca}_{25}\text{Zn}_{50}$ - $\text{Al}_{20}\text{Ca}_{25}\text{Zn}_{55}$) and IM3 ($\text{Al}_{15}\text{Ca}_{63}\text{Zn}_{22}$) were discovered in this system. The existence of two ternary compounds: C36 and Al_2CaZn_2 were confirmed. Their solubilities at 623 K were found to be: C36 ($\text{Al}_{58}\text{Ca}_{33}\text{Zn}_9$ - $\text{Al}_{43}\text{Ca}_{33}\text{Zn}_{24}$) and Al_2CaZn_2 ($\text{Al}_{55}\text{Ca}_{20}\text{Zn}_{25}$ - $\text{Al}_{40}\text{Ca}_{20}\text{Zn}_{40}$). These findings enhance the

understanding of the Al-Ca-Zn system and establish the phase relationships and solubility ranges between various phases.

Acknowledgments

Financial support from General Motors of Canada Ltd. and NSERC through the CRD grant program is gratefully acknowledged.

ACCEPTED MANUSCRIPT

References

- [1] W.T. Wang, X.M. Zhang, Z.G. Gao, Y.Z. Jia, L.Y. Ye, D.W. Zheng and L. Liu, *J. Alloys Compd.* 491(2010) 366-371.
- [2] Y.C. Tsai, C.Y. Chou, S.L. Lee, C.K. Lin, J.C. Lin and S.W. Lim, *J. Alloys Compd.* 487(2009) 157-162.
- [3] E. Parshizfard and S.G. Shabestari, *J. Alloys Compd.* 509(2011) 9654-9658.
- [4] Y. Deng, Z.M. Yin, K. Zhao, J.Q. Duan, Z.B. He, *J. Alloys Compd.* 530(2012) 71-80.
- [5] G. Piatti, G. Pellegrini and R. Trippodo, *J. Mater. Sci.* 11(1976) 186-190.
- [6] D.M. Moore and L.R. Morris, *Mater. Sci. Eng.* 43(1980) 85-92.
- [7] M.T. Perez-Prado, J. Ibanez, M.C. Cristina, M.A. Morris-Munoz, O.A. Ruano and G. Gonzalez-Doncel, *Mat. Trans.* 40(1999) 1011-1014.
- [8] V.A. Shvets, V.O. Lavrenko and V.M. Talash, *Mat. Sci.* 42(2006) 563-565.
- [9] N. Kono, Y. Tsuchida, S. Muromachi and H. Watanabe, *Light Met.* 35(1985) 574-580.
- [10] G. Cordier, E. Czech and H. Schafer, *Z Naturforsch B* 39B(1984) 1629-1632.
- [11] I.N. Ganiev, M.S. Shukroev and K.M. Nazarov, *Zh. Prikl. Khim.* 68(1995) 1646-1649.
- [12] I.N. Gantsev, K.M. Nazarov, M.M. Khakhdodov and N.I. Gantseva, *Evtpektika V, Mizhnarodna Konferentsiya, Dnepropetrovsk, National Metallurgical Academy of Ukraine, Dnepropetrovsk, Ukraine* (2000) 56-58.
- [13] M. Pani, L. Fornasini, D. Mazzone and F. Merlo, *Z. Kristallogr.* 224(2009) 397-406.
- [14] K. Söderberg, M. Bostrom, Y. Kubota, T. Nishimatsu, R. Niewa, U. Häussermann, Y. Grin, and O. Terasaki, *J. Solid. State. Chem.* 179(2006) 2690-2697.
- [15] M. Pani, L. Fornasini and F. Merlo, *Z. Kristallogr.* 222(2006) 218-225.
- [16] K. Söderberg, Y. Kubota, N. Muroyama, D. Grüner, A. Yoshimura and O. Terasak, *J. Solid. State. Chem.* 181(2008) 1998-2005.
- [17] M. Wendorff and C. Röhr, *Z Naturforsch. B* 62B(2007) 1549-1562.
- [18] S. Wasiur-Rahman, *Thermodynamic Modeling of the (Mg, Al)-Ca-Zn Systems*, M.A.Sc thesis in Mechanical and Industrial Engineering, (2009), Concordia University, Montreal, QC, Canada.
- [19] S. Wasiur-Rahman and M. Medraj, *CALPHAD* 33(2009) 584-598.
- [20] P. Villars and K. Cenzual, (2009) *Pearson's Crystal Data—Crystal Structure Database for Inorganic Compounds* (on CD-ROM) (Materials Park, OH: ASM International).

List of Figures Captions

Fig. 1. Graphical summary of the literature data.

Fig. 2. Back-scattered electron image of SSDC-1 annealed at 623 K for 5 weeks. (Al_1) denotes Al-rich fcc solid solution and (Al_2) denotes Zn-rich Al solid solution.

Fig. 3. Back-scattered electron image of SSDC-2 at 623 K annealed for 5 weeks.

Fig. 4. Back-scattered electron image of SSDC-3 at 623 K annealed for 5 weeks.

Fig. 5. Back-scattered electron image of SSDC-4 at 623 K annealed for 5 weeks.

Fig. 6. Backscattered electron image of solid-liquid diffusion couple Al₂Ca-Zn at 623 K annealed for 5 weeks. Points in brackets are offsets.

Fig. 7. Phase analysis of Al₁₃Ca₁₇Zn₇₀ sample using EPMA and XRD results.

Fig. 8. Phase analysis of key samples projected on the solid solubilities detected using diffusion couples.

Fig. 9. The pseudobinary Al₂Ca-CaZn₂ phase diagram constructed using data of Söderberg et al. [14] and our experimental data.

Fig. 10. The isothermal section of the Al-Ca-Zn system at 623 K.

List of Tables Captions

Table 1. Experimental solid solubilities in the Al-Ca-Zn system at 623 K.

ACCEPTED MANUSCRIPT

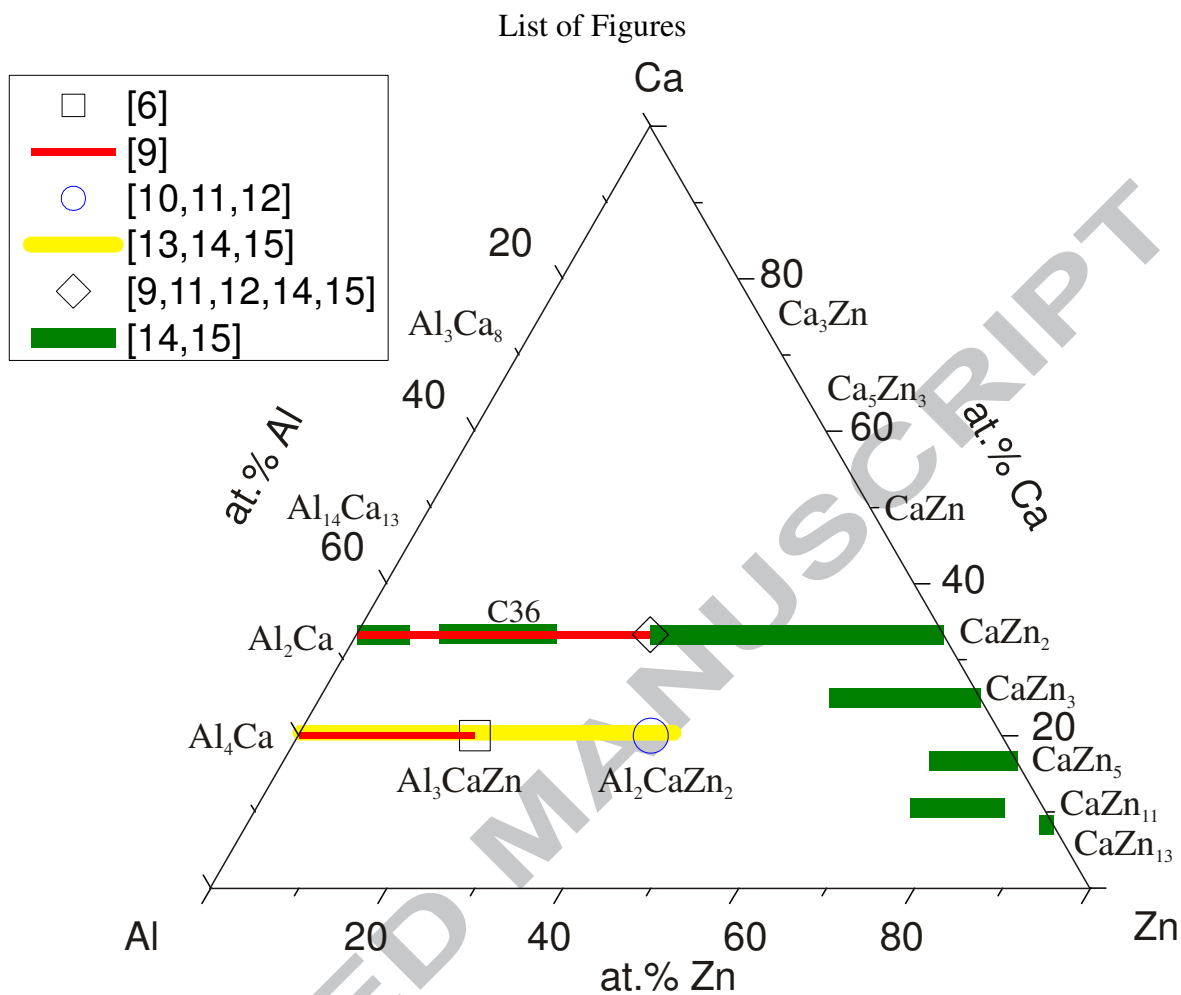


Fig. 1. Graphical summary of the literature data.

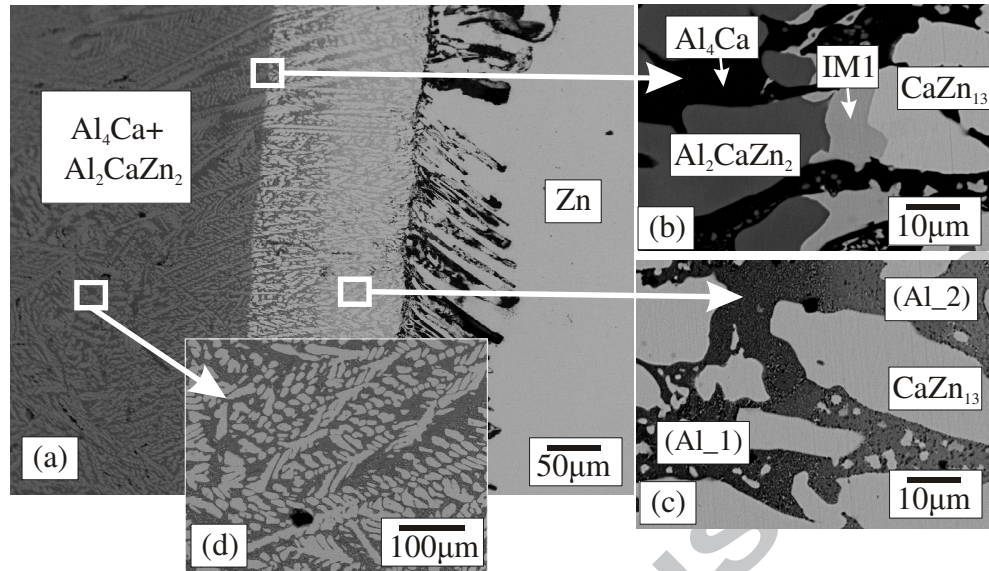


Fig. 2. Back-scattered electron image of SSDC-1 annealed at 623 K for 5 weeks.

(Al₁) denotes Al-rich fcc solid solution and (Al₂) denotes Zn-rich Al solid solution.

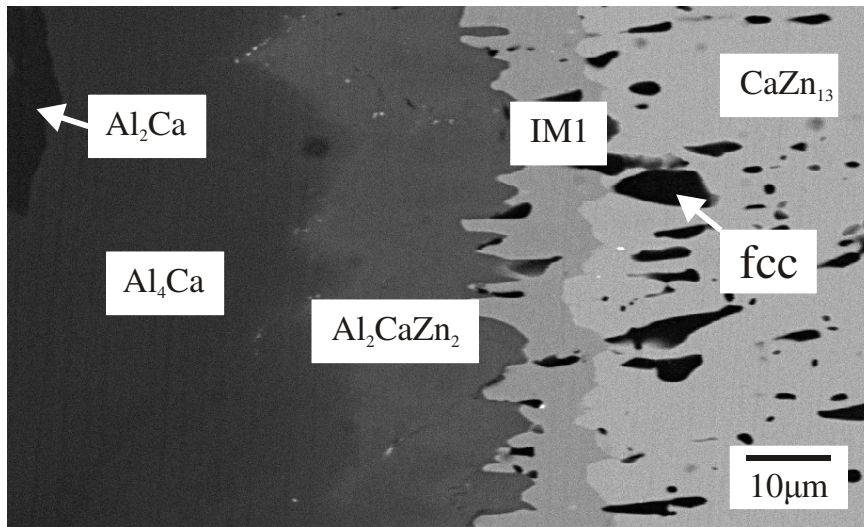


Fig. 3. Back-scattered electron image of SSDC-2 at 623 K annealed for 5 weeks.

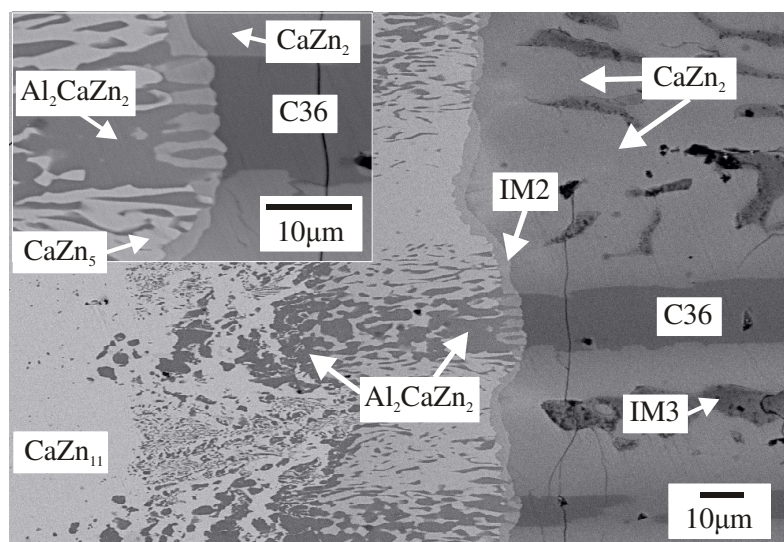


Fig. 4. Back-scattered electron image of SSDC-3 at 623 K annealed for 5 weeks.

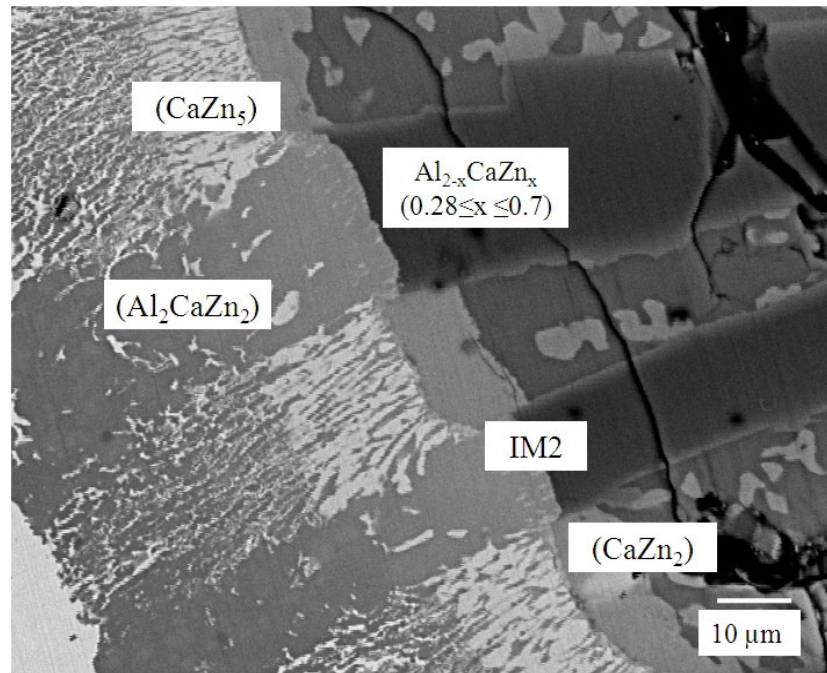


Fig. 5. Back-scattered electron image of SSDC-4 at 623 K annealed for 5 weeks.

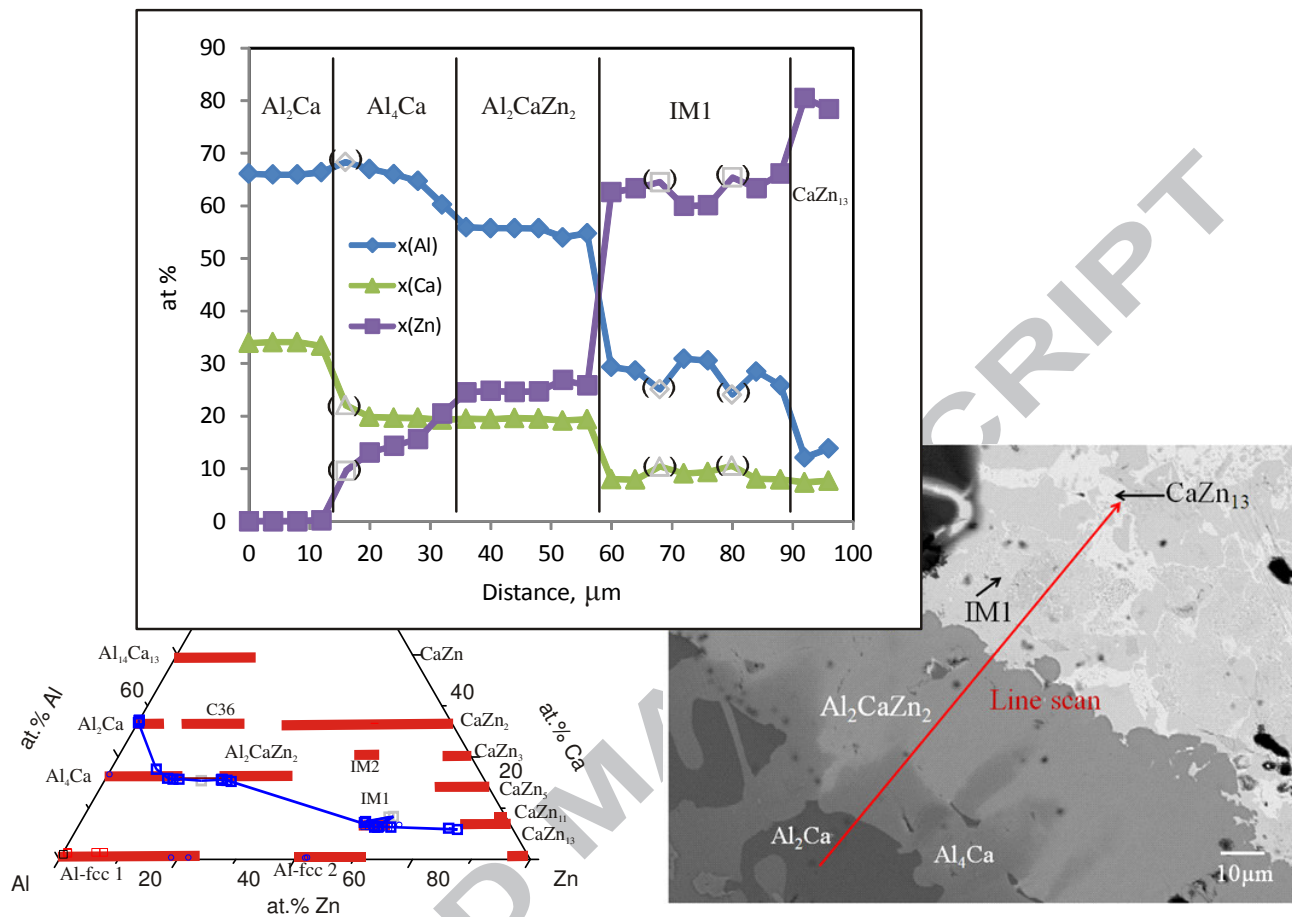


Fig. 6. Backscattered electron image of solid-liquid diffusion couple Al_2Ca -Zn at 623 K annealed for 5 weeks. Points in brackets are offsets.

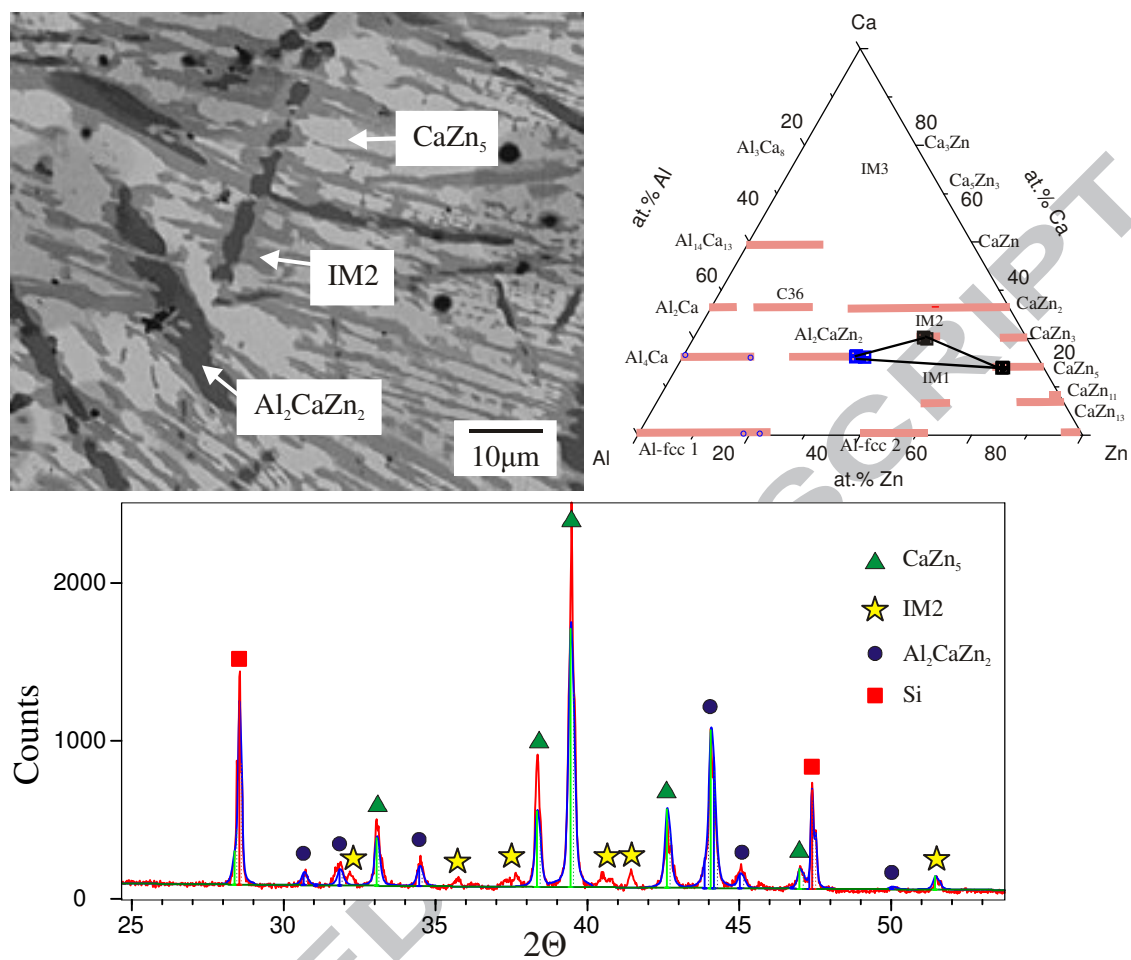


Fig. 7. Phase analysis of $\text{Al}_{13}\text{Ca}_{17}\text{Zn}_{70}$ sample using EPMA and XRD results.

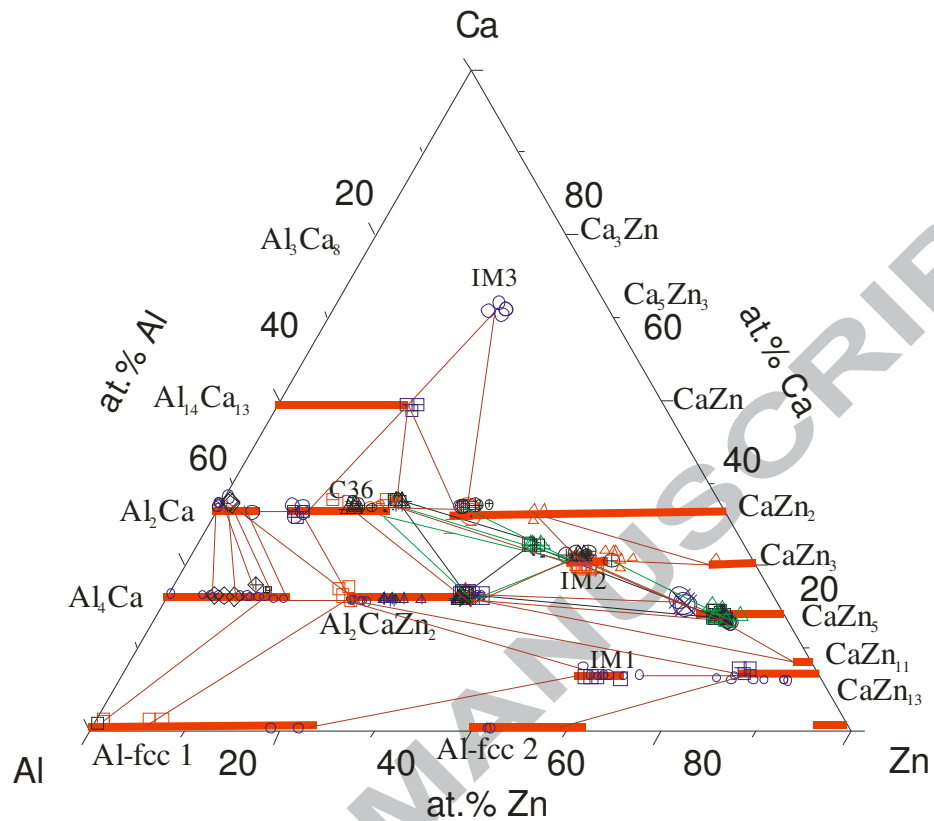


Fig. 8. Phase analysis of key samples projected on the solid solubilities detected using diffusion couples.

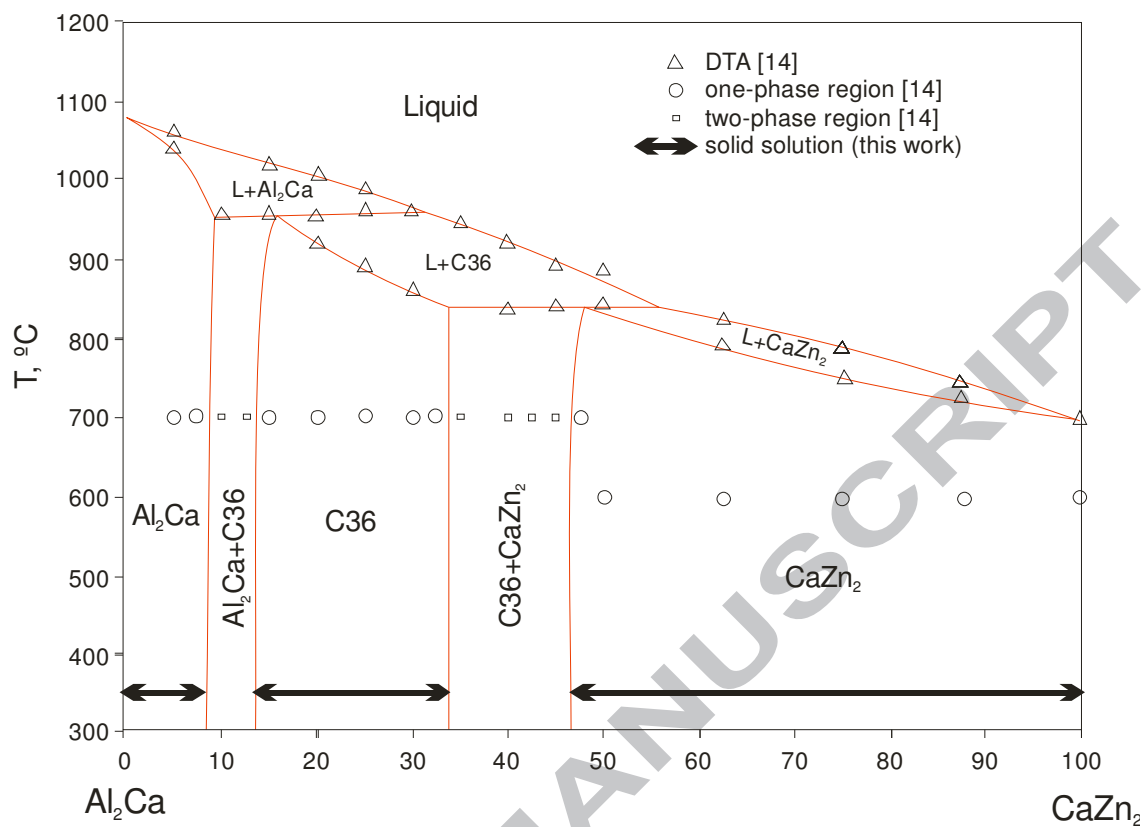


Fig. 9. The pseudobinary $\text{Al}_2\text{Ca}-\text{CaZn}_2$ phase diagram constructed using data of Söderberg et al. [14] and our experimental data.

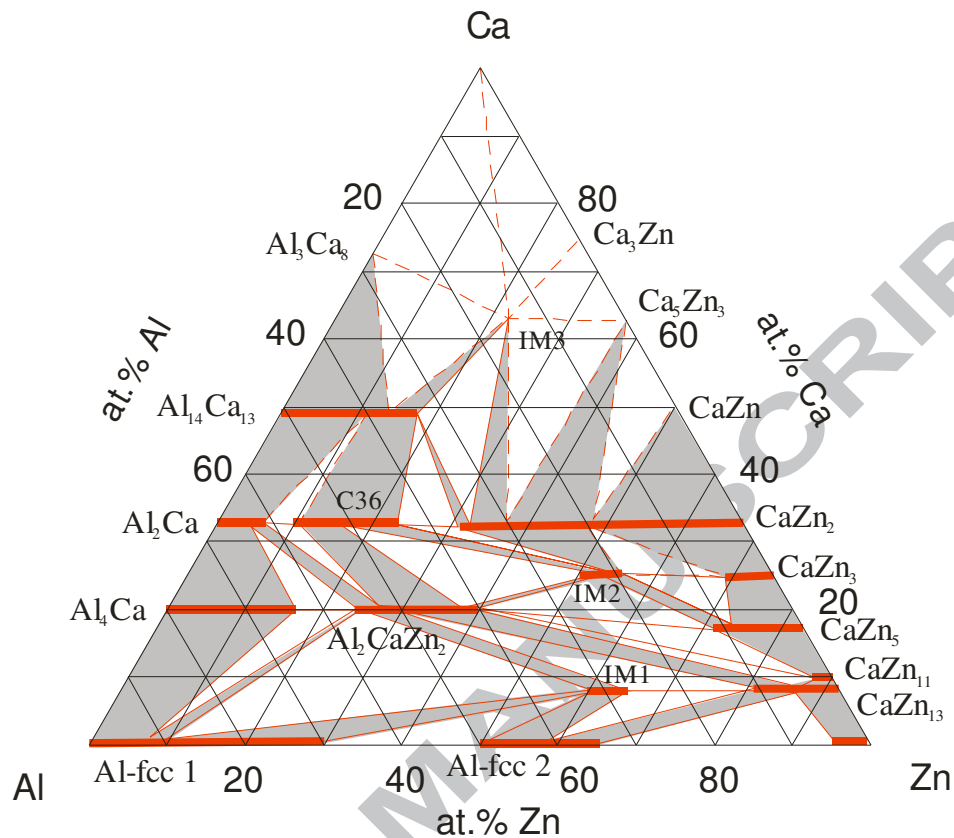


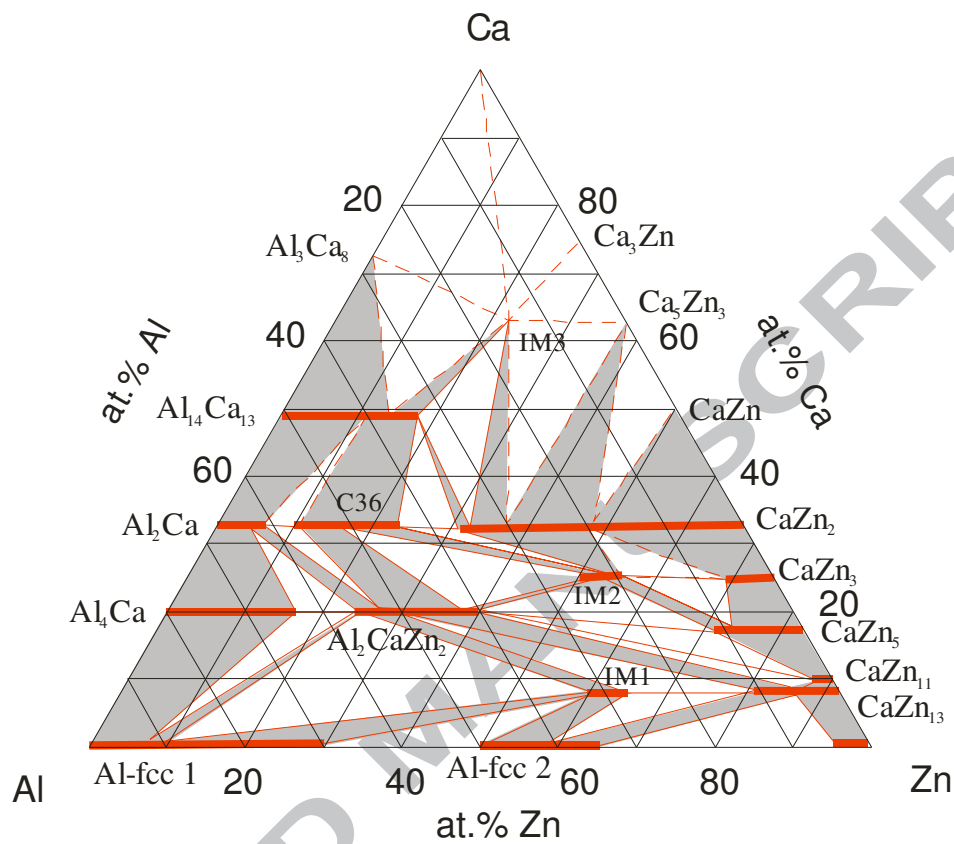
Fig. 10. The isothermal section of the Al-Ca-Zn system at 623 K.

List of Tables

Table 1. Experimental solid solubilities in the Al-Ca-Zn system at 623 K.

Compound	Start	End
Al₄Ca	Al ₈₀ Ca ₂₀	Al ₆₄ Ca ₂₀ Zn ₁₆
Al₂Ca	Al ₆₆ Ca ₃₃	Al ₆₀ Ca ₃₃ Zn ₆
Al₁₄Ca₁₃	Al ₅₂ Ca ₄₈	Al ₃₄ Ca ₄₈ Zn ₁₈
CaZn₁₃	Al ₁₁ Ca ₇ Zn ₈₂	Ca ₇ Zn ₉₃
CaZn₁₁	Al ₂ Ca ₈ Zn ₉₀	Ca ₈ Zn ₉₂
CaZn₅	Al ₁₀ Ca ₁₇ Zn ₇₃	Ca ₁₇ Zn ₈₃
CaZn₃	Al ₆ Ca ₂₅ Zn ₆₉	Ca ₂₅ Zn ₇₅
CaZn₂	Al ₃₁ Ca ₃₃ Zn ₃₆	Ca ₃₃ Zn ₆₇
C36	Al ₅₈ Ca ₃₃ Zn ₉	Al ₄₃ Ca ₃₃ Zn ₂₄
Al₂CaZn₂	Al ₅₅ Ca ₂₀ Zn ₂₅	Al ₄₀ Ca ₂₀ Zn ₄₀
IM1	Al ₃₀ Ca ₈ Zn ₆₂	Al ₂₇ Ca ₈ Zn ₆₅
IM2	Al ₂₅ Ca ₂₅ Zn ₅₀	Al ₂₀ Ca ₂₅ Zn ₅₅
IM3	Al ₁₅ Ca ₆₃ Zn ₂₂ stoichiometric compound	

Graphical Abstract



The isothermal section of the Al-Ca-Zn system at 623 K

Highlights

- The isothermal section of the Al-Ca-Zn phase diagram at 350°C was constructed.
- The homogeneity ranges of ternary and binary compounds have been determined.
- Three new ternary compounds (IM1, IM2 and IM3) have been found and the existence of two ternary compounds (C36 and Al_2CaZn_2) has been confirmed.
- This study enhanced the understanding of the Al-Ca-Zn ternary phase diagram and established the phase relationships and solubility ranges between various phases.

ACCEPTED MANUSCRIPT